

# Numerical investigation on the effects of cavity on fluid flow and heat transfer characteristics in rectangular microchannel heat sink (MCHS).

Dipak Debbarma<sup>1</sup>, Sunita Debbarma<sup>2</sup>, Siddhartha Das<sup>3</sup>,  
Bijoy Kumar Deb<sup>4</sup>, Biswajit Datta<sup>5</sup>

<sup>1,4</sup> (Department of Mechanical Engineering, Tripura Institute of Technology, India)

<sup>2</sup> (Department of Computer Science and Technology, Women's Polytechnic, Tripura, India)

<sup>3,5</sup> (Department of Automobile Engineering, Tripura Institute of Technology, India)

## Abstract

*This work represents the results of channel with cavity mounted on both sidewalls. The cavities are used on the both sidewalls of the rectangular microchannel to study the fluid flow and heat transfer behavior of micro-channel heat sink. The channel studied is the channel with 10 no cavities mounted on both sidewalls. The cavity parameters considered are  $D_{cav} = 50 \mu\text{m}$  and  $W_{cav} = 150 \mu\text{m}$ , which are the optimum parameters as found in the earlier work of this author. The present study is carried out for the  $Re$  of range from 206 to 610.*

*The presence of cavity plays important role in the performance characteristics of microchannel. An important observation of the study is that a number of cavity causes lower average channel temperature, better temperature distribution which leads to enhanced Nusselt number  $Nu$  as well as heat transfer enhancement factor ( $\eta$ ).*

**Keywords :** Cavity, heat transfer enhancement factor, friction factor, vortices.

## 1. Introduction

Improvement of microchannel heat sink in terms of heat transfer enhancement is very essential to meet the demand of present trends of technology. The performance of the modern electronics system especially micro-electro mechanical system is dependent on the cooling capacity of microchannel. Hence, it is appreciated to innovate appropriate technique which enable higher heat removal for better cooling.

Tuckerman and Pease [1] first explained the concept of microchannel heat sinks, in early 1981, by the investigation of high-performance forced liquid cooling of integrated circuits. In a series of experiments, they evaluated the optimum design variables for  $Re = 730$ , which causes minimum total thermal resistance. They could observe the maximum heat flux of  $790 \text{ W/cm}^2$ . Since then, the researchers started works on microchannel and subsequently many techniques are developed by them to enhance the heat transfer capacity.

Xia et al. [2] studied the microchannel with aligned fan-shaped reentrant cavities taking water as cooling fluid for Reynold's number ranged 132-931. The influences of constant cross-section region and arcuate region parameters on heat transfer were investigated by them. They observed that when the number of the reentrant cavities is smaller, the combined effect is too weak to affect the fluid flow. With the increase in the number of the reentrant cavities the combined effect becomes strong. Xia et al. [3] found the optimum geometric parameters based on sidewall of microchannel with triangular cavity, by a numerical study. They studied the effects of these parameters on heat transfer enhancement factor and Nusselt number ratio ( $Nu/Nu_0$ ). They got good enhancement due to the vortices formed which diminished laminar stagnation zones in the corner. Chai et al. [4] investigated numerically the effects of flow rate and heat flux on pressure drop and heat transfer in a microchannel heat sink with offset fan-shaped reentrant cavities in sidewall and compared them with the result of the corresponding conventional rectangular microchannel heat sink. They observed that the effect of flow rate is such that the heat transfer increases substantially with the increase of flow rate. Chai et al. [5] performed both experimental and numerical investigations to study the influences of periodic expansion–contraction cross sections on pressure drop, heat transfer and thermal resistance in microchannel. They compared the results of fan-shaped reentrant cavities, triangular-shaped reentrant cavities and the channel without cavity. In the study of  $Nu$  versus  $Re$ , it was observed that the  $Nu$  is significantly increasing with the increase of  $Re$  for all types of microchannel. Kuppusamy et al. [6] conducted numerical study in triangular grooved microchannel heat sink using nanofluid. Their study showed that with the increment of angle ( $\theta$ ) and depth ( $d$ ) the thermal enhancement is augmented because of the increase in fluid–solid interface area and vortices. Ahmed and Ahmed [7] investigated the grooved microchannel heat sinks and optimized the design of the cavity shape. They compared the effect of groove of triangular, trapezoidal and rectangular shape formed by changing the value of groove tip length ratio ( $\phi$ ). They observed that the groove shape trapezoidal is the best for enhancement in the heat transfer at  $Re = 100$ . The effects of other parameters such as groove depth ratio, pitch ratio, orientation ratio were also studied. The work on microchannel with zigzag grooves on sidewall by Ma et al. [8] showed that the zig-zag not very long and not much short results in good enhancement in heat transfer due to the interruption of the periodic thermal boundary layer along the flow direction.

Chai et al. [9] performed numerical investigations to study thermal and hydraulic characteristics of laminar flow in microchannel heat sink with fan-shaped ribs on sidewalls. The geometric parameters include the width  $W_r$  (0.05–0.4 mm), height  $H_r$  (0.005–0.025 mm) and spacing  $S_r$  (0.2–5 mm) of aligned or offset fan-shaped ribs. The highest number (50) ribs in 10 mm channel causes the large interruption of streamlines which provides heat transfer enhancement. Chai et al. [10] studied numerically the effects of geometry of fan rib on friction factor of MCHS in the part 2 of the earlier investigation Chai et al. [9].

The use of cavity in microchannel shows better result with significant heat transfer enhancement factor. The aim of the present paper is to find the effects of number of cavity on fluid flow and heat transfer characteristics used on the sidewalls of channel.

## 2. Numerical modeling of microchannel heat sink

The rectangular microchannel with cavities on both sidewalls are simulated in the present study. The microchannel without cavity i.e. rectangular plain channel is compared with the results of the study. Water is flowing through a rectangular micro channel. The overall dimensions of plate is with width = 10 mm, Length = 20 mm and Height = 0.35 mm.

In this study, a single micro channel out of 10 channels is considered as computational domain. Figure 2.1 represents the unit cell (computational domain) of plain rectangular micro channel heat sink. Dimension of unit cell micro channel are shown below:  $W_c = 0.1$  mm and  $D_c = 0.2$  mm.

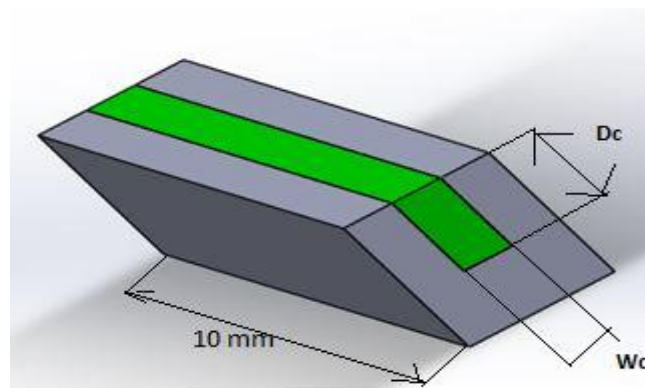


Figure 2.1 : Computational domain of rectangular plain channel

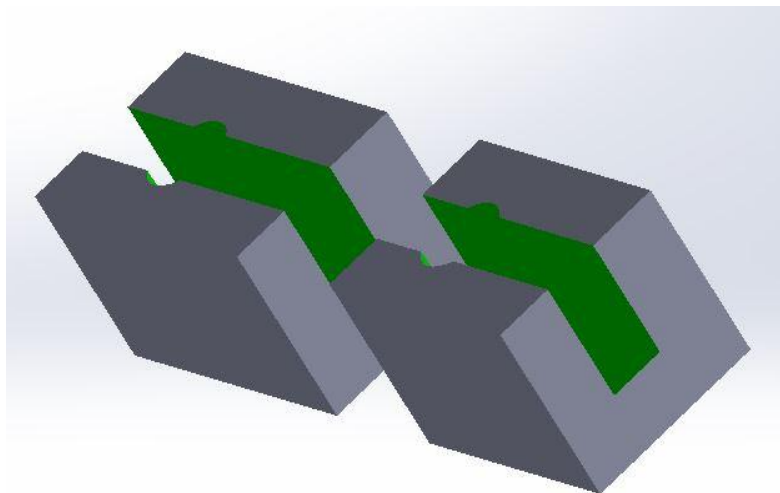


Figure 2.2 : A Channel section with cavity

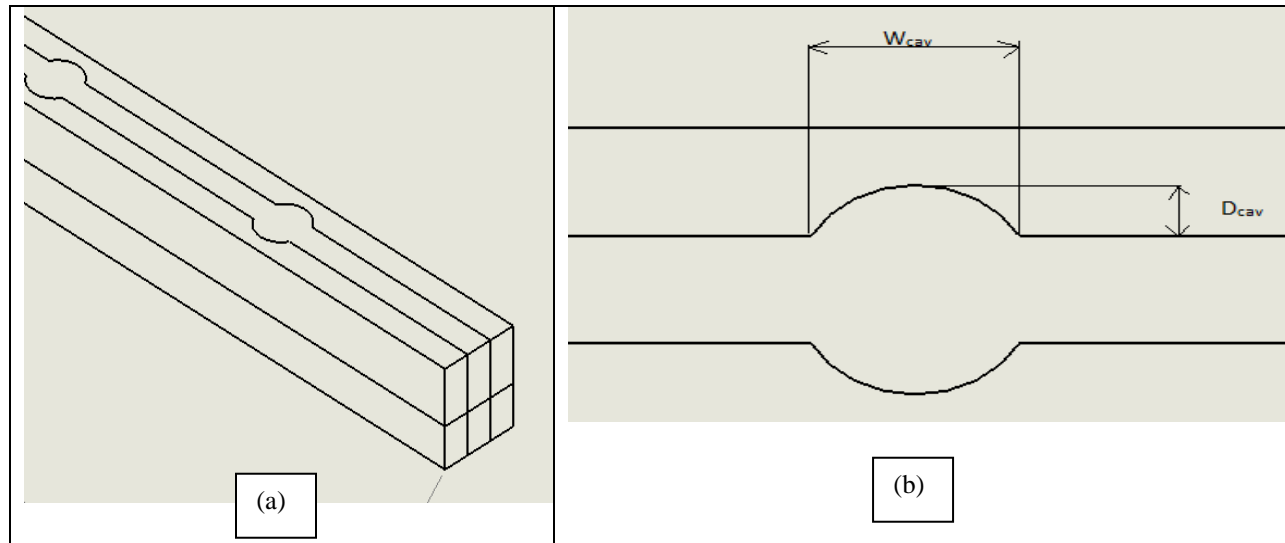


Figure 2.3 : (a) A Channel section with cavity, (b) A Cavity with depth  $D_{cav}$  and width  $W_{cav}$

### 3. Mathematical formulation

#### 3.1 Governing equations

The fundamental governing equations are given below:

Mass conservation equation:

$$\frac{\partial u}{\partial x} + \frac{\partial v}{\partial y} + \frac{\partial w}{\partial z} = 0 \quad (1)$$

Momentum conservation equations:

$$\frac{\partial u}{\partial t} + \frac{\partial(uu)}{\partial x} + \frac{\partial(uv)}{\partial y} + \frac{\partial(uw)}{\partial z} = \nu(\frac{\partial^2 u}{\partial x^2} + \frac{\partial^2 u}{\partial y^2} + \frac{\partial^2 u}{\partial z^2}) - (1/\rho)(\partial p/\partial x) \quad (2)$$

$$\frac{\partial v}{\partial t} + \frac{\partial(vu)}{\partial x} + \frac{\partial(vv)}{\partial y} + \frac{\partial(vw)}{\partial z} = \nu(\frac{\partial^2 v}{\partial x^2} + \frac{\partial^2 v}{\partial y^2} + \frac{\partial^2 v}{\partial z^2}) - (1/\rho)(\partial p/\partial y) \quad (3)$$

$$\frac{\partial w}{\partial t} + \frac{\partial(wu)}{\partial x} + \frac{\partial(vw)}{\partial y} + \frac{\partial(ww)}{\partial z} = \nu(\frac{\partial^2 w}{\partial x^2} + \frac{\partial^2 w}{\partial y^2} + \frac{\partial^2 w}{\partial z^2}) - (1/\rho)(\partial p/\partial z) \quad (4)$$

#### 3.2 Boundary conditions

In the micro-scale fluid flow, different flow regimes would be there depending on the value of Knudsen number

( $K_n$ ) [5], which is given by :

$$K_n = \lambda/d_h \quad (5)$$

Where  $\lambda$  is mean free path of fluid molecules.

The Knudsen number ( $K_n$ ) is used to calculate whether the fluid is considered as continuum and for the flow which follows continuum, Navier-Stokes equations would be applied [5]. If the Knudsen number ( $K_n$ ) is less than

$10^{-3}$  no slip condition is adopted. In the present study, Knudsen number ( $K_n$ ) for water under the conditions is less than  $10^{-3}$ . So no slip boundary condition is assigned for the surfaces.

At the inlet, the inlet temperature,  $T_{in} = 293K$  and the uniform heat flux applied at bottom surface,  $q = 1 \times 10^6$  W/m<sup>2</sup>.

### 3.3 Associated equations

(i) The Reynolds number : Re is given as below

$$Re = \rho u_m d_h / \mu \quad (6)$$

Where  $\rho$  is the fluid density,  $u_m$  is the average flow velocity,  $d_h$  is the hydraulic diameter and  $\mu$  represents the fluid viscosity.

(ii) The hydraulic diameter ( $d_h$ ) : It is defined by

$$d_h = (2W_c D_c) / (W_c + D_c) \quad (7)$$

Where  $W_c$  = Channel Width,  $D_c$  = Channel height = channel depth

[iii] The average apparent friction factor ( $f$ ):  $f$  is computed by pressure drop ( $\Delta p$ ) across the length of the micro-channel ( $L$ ) as,

$$f_{app,ave} = f = (2\Delta p d_h) / (\rho u_m^2 L) \quad (8)$$

Where  $L$  = length of the micro-channel.

[iv] Nusselt number:  $Nu$  is given by

$$Nu = h d_h / k \quad (9)$$

where  $h$  = heat transfer coefficient of fluid and  $k$  = thermal conductivity of fluid.

[v] The average heat transfer coefficient ( $h$ ) is obtained from the following expression :

$$h = q A_b / (A_{con} (T_b - T_{int})) \quad (10)$$

Where  $q$  = heat flux per area,  $A_b$  = Bottom wall area through which heat is given,  $A_{con}$  = convection heat removal area which is the actual surface area of channel considering two sidewall and bottom wall,  $T_b$  = average temperature of bottom wall,  $T_{int}$  = average temperature of interior part of the channel.

[vi] The thermal enhancement factor ( $\eta$ ) is given by

$$\eta = \frac{h}{h_0} \bigg|_{pp} = \frac{Nu}{Nu_0} \bigg|_{pp} = (Nu/Nu_0) / (f/f_0)^{(1/3)} \quad (11)$$

where  $Nu_0$  and  $f_0$  stand for Nusselt number and friction factor for the straight microchannel, respectively.

Water is taken as working fluid for the investigation. So the properties of water are the properties of the fluid material. Silicon is considered as the substrate material for the investigation.

## 4. Numerical solution

### 4.1 Numerical method

For the numerical simulation, the implicit method is to be adopted for the governing equations discretization; the second order upwind scheme is used for discretizing the convective terms in the momentum and energy conservation equations. The SIMPLEC method is adopted in the Fluent solver.

### 4.2 Grid independency test

To ensure that the present simulation solution is independent of grid size, validation test is carried out on models. As per the simulation results, the relative errors is less than 0.55% for the grid size of 1.3 million in comparison to the grid systems with 2.7 millions cells for the models of Smooth Rectangular. And the grid system with 1.1 million, adopted for channel with cavity, would predict best accuracy with less error.

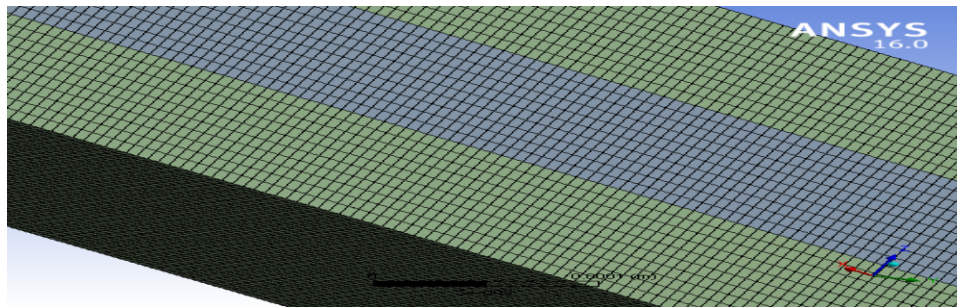


Figure 4.1 : Meshed model of rectangular plain channel

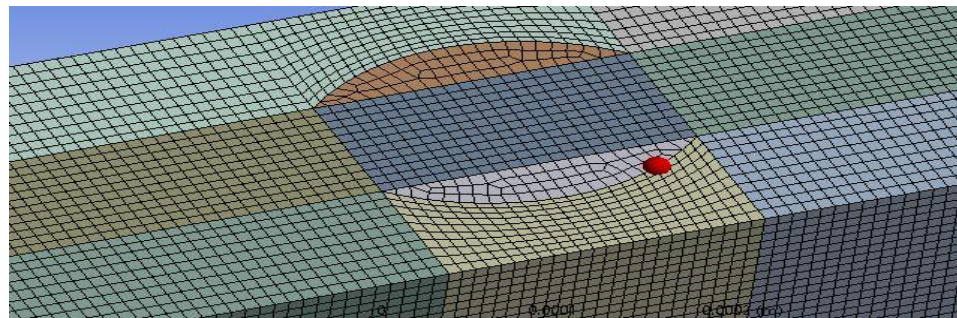


Figure 4.2 : Meshed model of channel with cavity

## 5. RESULTS AND DISCUSSION

### 5.1 Validation of numerical solution method

The results of the present study are in well agreement with that of both experimental and numerical study by Chai et al.(2013) [5], with an average deviation of maximum 1.65 % in  $Nu$ . Therefore the present numerical method and model ensure the reliability and accuracy of the solution results.

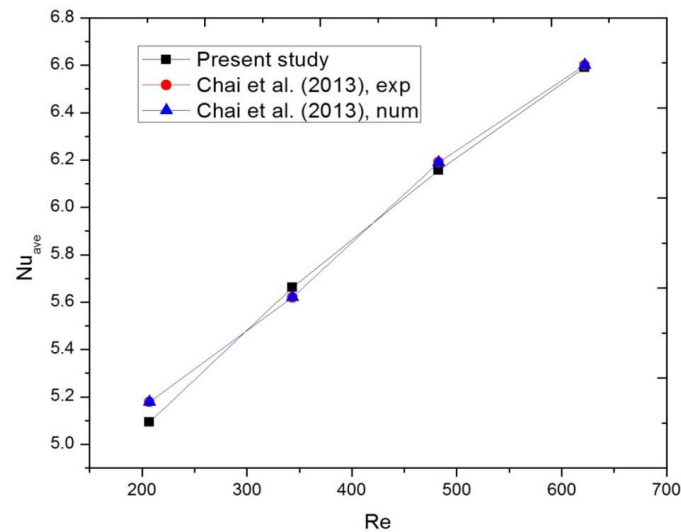


Figure 5.1 : Comparison of  $Nu$  between present study and Chai et al.(2013) [5]

## 5.2 Fluid flow characteristics

The channel studied in the present is the channel with 10 no cavity mounted on both sidewalls. The cavity parameters are as  $D_{cav} = 50 \mu m$  and  $W_{cav} = 150 \mu m$ , which are the optimum parameters as found in the earlier work of this author.

Fig. 5.2 shows the velocity distribution of plain channel and channels with cavity, simulated at inlet velocity of 4 m/s. The distributions are for the horizontal sectional planes at the centre of channel at a height of  $100 \mu m$  from the base of liquid channel. It is found that the water flow velocity at the entrance of the cavity decreases dramatically due to sudden expansion of the flow area. A stagnation zone of flow is formed inside the cavity. The fluid particles in that stagnation zone can be flown along with the mainstream.

Fig. 5.3 shows the pressure distribution of plain channel and channel with cavities. Li et al. [4] observed that the static pressure reduces gradually as the water flows along the longitudinal direction of the channel for the cavity channel, which has also been found in the present study. The upstream region of cavity is subjected to lower pressure and lower velocity whereas the higher pressure is created in the downstream i.e. end of cavity as shown in the figure of pressure distribution.

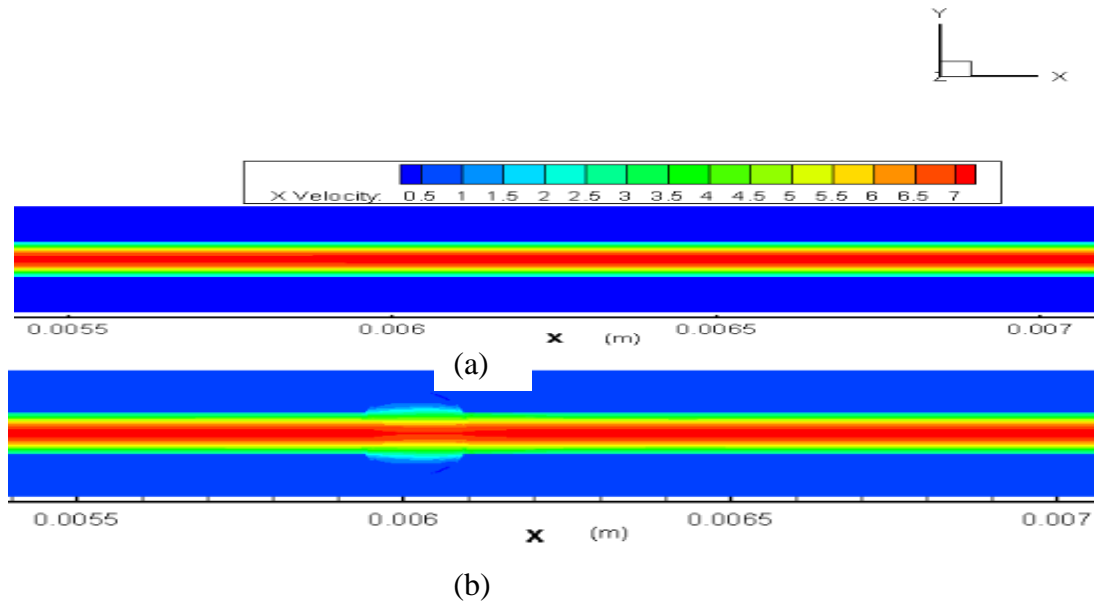


Figure 5.2 : Velocity distribution in x - direction for (a) Plain channel, (b) channel with 10 no cavity ( $D_{cav} = 50 \mu m$  and  $W_{cav} = 150 \mu m$ )

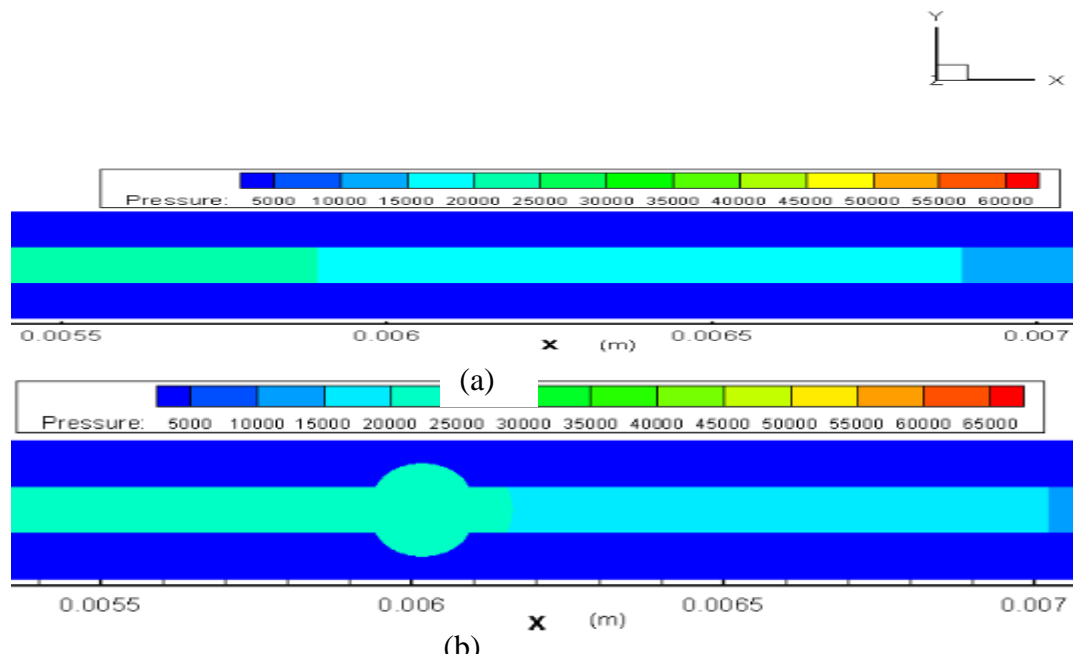


Figure 5.3 : Pressure distribution in x - direction for (a) Plain channel, (b) channel with 10 no cavity ( $D_{cav} = 50 \mu m$  and  $W_{cav} = 150 \mu m$ )

### 5.3 Heat transfer characteristics

Fig. 5.4 shows the temperature distribution in x - direction for Plain channel and channel with cavity, simulated at inlet velocity of 4 m/s. The distributions are for the horizontal sectional planes at the centre of channel at a height of 100  $\mu m$  from the base of liquid channel. The temperature distribution of the channel studied is better than that of

plain channel. At inlet fluid velocity of 4 m/s, the average temperature is 298.79 for the channel. The less average temperature of fluid is the result of thermal boundary layer interruption, intense fluids mixing. Similar observation was described by Xia et al. [3]. They stated that the vortices in the reentrant cavity bring chaotic advection and enhance the convective fluid mixing. The lateral mixing disrupts the shear layer separating the bulk flow and the recirculating flow in the reentrant cavity, therefore, leads to heat transfer enhancement without any external forces.

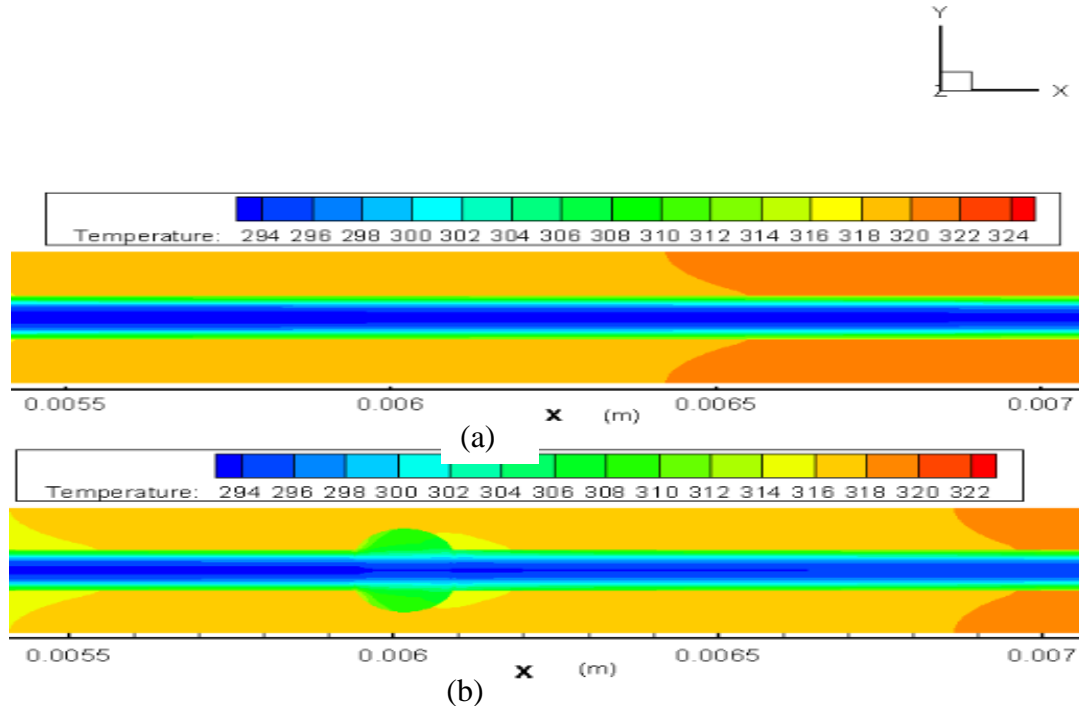


Figure 5.4 : Temperature distribution in x - direction for (a) Plain channel, (b) channel with 10 no cavity ( $D_{cav} = 50 \mu m$  and  $W_{cav} = 150 \mu m$ ).

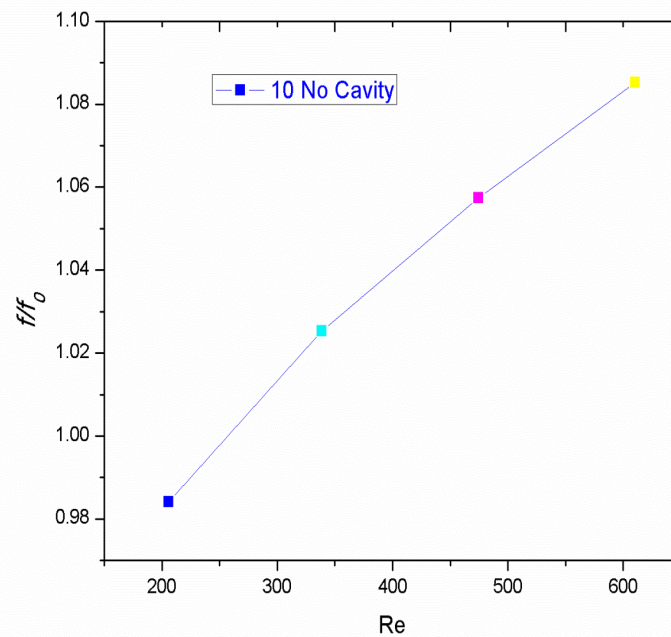
In earlier work of this Author, it is observed that the microchannel with depth of  $50 \mu m$  shows better  $Nu/Nu_o$  than the channels with other depth for the same cavity width of  $150 \mu m$ . The shape of the vortices formed into the cavity and fluid velocity are the factors which cause rise in  $Nu/Nu_o$  for the channel. The pressure peak value appears at the frontal face of the contraction segment and the reverse pressure gradient occurs along the sidewall leading to the formation of vortices into the cavity. The suitable shape and intensity of the vortices introduce the proper mixing of the fluids into the cavity. As result, convection heat transfer is increased and consequently  $Nu$  is increased.

Fig. 5.5(c) shows the comparison of heat transfer enhancement factor ( $\eta$ ) for channel with 10 umber cavity. The relationship between the heat transfer enhancement and pressure drop is justified by the term heat transfer enhancement factor ( $\eta$ ) which is given by,

$$\eta = (Nu/Nu_o)/(f/f_o)^{(1/3)}$$

The cavity cross-section of the microchannel of Chai et al. [5] has significant influence on temperature field, which enables better fluid mixing between the wall and core flow regions. For this channel,  $Nu/Nu_o$  is significantly increasing at higher Re. The heat transfer enhancement factor ( $\eta$ ) is also having the highest value at largest Re. It is 1.28 at Re 610.

The rise in  $Nu/Nu_o$  is possible at the cost of higher pressure drop. The ratio  $Nu/Nu_o$  is 1.116329 at Re 206 and reaches to the highest value of 1.317959 at Re 610. The value of  $f/f_o$  is 0.984148 and 1.08518 for the corresponding value of Re. This signifies that presence of the cavities on the sidewall of microchannel increases the surface area and helps in better mixing of fluid which causes the enhancement in  $Nu$  as well as the heat transfer enhancement factor ( $\eta$ ).



(a)

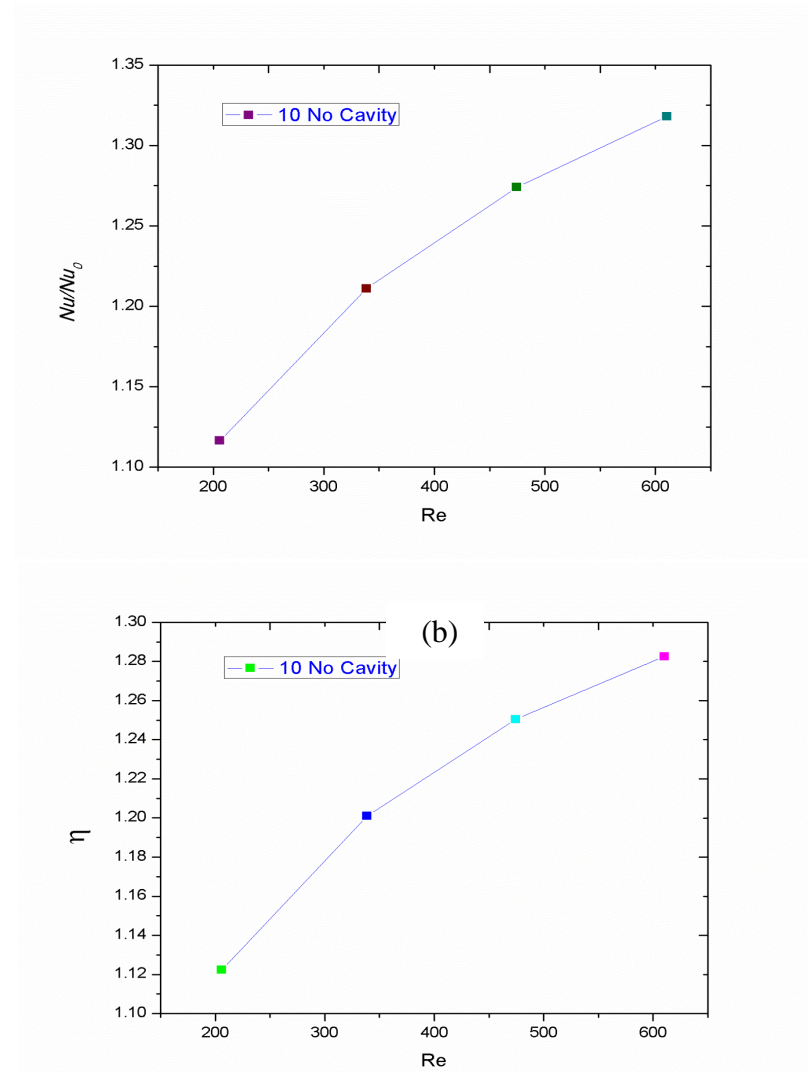


Figure 5.5 : (a) Comparison of Nusselt number ratio ( $Nu/Nu_o$ ), (b) Comparison of friction factor ratio ( $f/f_o$ ), (c) Comparison of heat transfer enhancement factor ( $\eta$ ) of the microchannel at different Re.

## 6. CONCLUSION

(c)

1. In the analysis, it is observed that the microchannel with cavity shows better result in terms of fluid flow and heat transfer characteristics than the plain channel.
2. The lower average channel temperature indicates that the better heat transfer occurs from the water thereby enhancing Nusselt number. Higher inlet velocity and larger number of cavity attribute frequent boundary layer interruption and redevelopment, lower average channel temperature, better fluids mixing, enhanced Nusselt number. At the maximum  $Re = 610$ , the ratio  $Nu/Nu_o$  is 1.317959 for the microchannel with 10 number cavity and the  $Nu$  is 8.68.

3. The heat transfer enhancement factor ( $\eta$ ) is also having the highest value at the largest Re. It is 1.28 at Re 610. This signifies that presence of the cavities on the sidewall of microchannel increases the surface area and helps in better mixing of fluid which causes the enhancement in  $Nu$  as well as the heat transfer enhancement factor ( $\eta$ ).

## REFERENCES

- [1] Tuckerman, D. B., and Pease, R. F. W., High-Performance Heat Sinking for VLSI, IEEE Electronic device letters, v. 2, NO. 5, 1981, pp. 126-129.
- [2] Xia, G.D., Chai, L., Zhou, M., Wang, H., Effects of structural parameters on fluid flow and heat transfer in a microchannel with aligned fan-shaped reentrant cavities, International Journal of Thermal Sciences, v. 50, 2011, pp. 411- 419.
- [3] Xia, G.D., Chai, L., Wang, H., Zhou, M., Cui, Z. Optimum thermal design of microchannel heat sink with triangular reentrant cavities, Applied Thermal Engineering, v. 31, 2011, pp. 1208-1219.
- [4] Chai, L., Xia G.D., Zhou, M., Li, J., Numerical simulation of fluid flow and heat transfer in a microchannel heat sink with offset fan-shaped reentrant cavities in sidewall, International Communications in Heat and Mass Transfer, v. 38, 2011 , pp. 577–584.
- [5] Chai, L., Xia, G.D., Wang, L., Zhou, M., Cui, Z., Heat transfer enhancement in microchannel heat sinks with periodic expansion–constriction cross-sections, International Journal of Heat and Mass Transfer, v. 62, 2013 , pp. 741–751.
- [6] Kuppusamy, N. R., Mohammed H.A., Lim C.W. Thermal and hydraulic characteristics of nanofluid in a triangular grooved microchannel heat sink (TGMCHS), Applied Mathematics and Computation, v.246, 2014, pp.168–183.
- [7] Ahmed, H.E., Ahmed, M. I. Optimum thermal design of triangular, trapezoidal and rectangular grooved microchannel heat sinks, International Communications in Heat and Mass Transfer, 2015.
- [8] Ma, D.D. , Xia , G.D. , Li, Y.F. , Jia, Y.T. , Wang J. , Effects of structural parameters on fluid flow and heat transfer characteristics in microchannel with offset zigzag grooves in sidewall, International Journal of Heat and Mass Transfer, v. 98, 2016, pp. 17–28.
- [9] Chai, L., Xia, G. D., Wang, H. S. ,Parametric study on thermal and hydraulic characteristics of laminar flow in microchannel heat sink with fan-shaped ribs on sidewalls – Part 1: Heat Transfer, International Journal of Heat and Mass Transfer, 2016.
- [10] Chai, L., Xia, G. D., Wang, H. S, Parametric study on thermal and hydraulic characteristics of laminar flow in microchannel heat sink with fan-shaped ribs on sidewalls – Part 2: Pressure drop, International Journal of Heat and Mass Transfer, 2016.

### Nomenclature

$D_h$	Hydraulic diameter of microchannel
$\eta$	Heat transfer enhancement factor
$u_m$	Average flow velocity
$\mu$	Fluid viscosity
$\nu$	Fluid kinematic viscosity
$\rho$	Fluid density
$L$	Length of the micro-channel
$W$	Channel Width
$H$	Channel height
$f_{app,ave}$	Average apparent friction factor
$\alpha_c$	Aspect ratio of channel
$\Delta p$	Pressure drop
$h$	Heat transfer coefficient of fluid
$h_0$	Heat transfer coefficient of fluid for plain channel
$k$	Thermal conductivity of fluid
$f$	Friction factor of microchannel
$f_0$	Friction factor of plain microchannel
$Nu$	Nusselt number of microchannel
$Nu_0$	Nusselt number of plain microchannel
$q$	Uniform heat flux
$W_c$	Width of the channel
$D_c$	Depth of the channel
$c_p$	Fluid specific heat
$A_b$	Bottom wall area through which heat is given
$A_{con}$	Convection heat removal area
$T_b$	Average temperature of bottom wall,
$T_{int}$	Average temperature of interior part of the channel.
$W_{cav}$	Width of the circular cavity
$D_{cav}$	Depth of the circular cavity
$\partial$	Design variable denoted by Xia et al.
$\theta$	Cavity angle denoted by Kuppusamy et al.
$d$	Cavity depth denoted by Kuppusamy et al.
$W_r$	Rib width
$H_r$	Rib height
$S_r$	Rib spacing
$e/D_h$	Relative rib height
$\alpha$	Relative rib width denoted by Li et al.
$D$	Diameter of dimples, protrusion
$\delta/D$	Relative depth denoted by Li et al.